DOI:10.1190/1.1845123

Increasing horizontal resolution of geophysical models by generalized inversion

Jianghai Xia, Richard D. Miller, Kansas Geological Survey, The University of Kansas;*
Chao Chen, China University of Geosciences; and
Julian Ivanov, Kansas Geological Survey, The University of Kansas

Summary

The horizontal resolution of a geophysical model is normally limited by the distance between a source and receivers of a seismic survey or a transmitter and receivers of an electromagnetic/electrical survey. This is because these surveys usually measure the average value of a physical property between the source and a receiver. For example, the Multichannel Analysis of Surface Waves (MASW) technique has been employed to generate 2-D shear (S)-wave velocity sections. The S-wave velocities of 2-D sections are average values of materials between the source and the last receiver. Interpretation based on the average model obviously generates low-quality products. Low horizontal resolution of the S-wave velocity models severely limits the potential application of MASW in near-surface geophysics. We discuss the inverse problem related to the average model and how to apply the generalized inversion to obtain a horizontal-resolution-improved model. A real-world example of the MASW technique demonstrates the increased horizontal resolution derived from the generalized inversion.

Introduction

A technique (Park et al., 1999, Xia et al., 1999) utilizing a multichannel recording system to estimate near-surface S-wave velocity from high-frequency (≥ 2 Hz) Rayleigh waves (Multichannel Analysis of Surface Waves—MASW) has been applied to more and more near-surface problems (e.g., Xia et al., 1998, 2002a, 2002b, and 2004; Ivanov et al., 2000; Miller et al., 1999; Yilmaz and Eser, 2002; Calderon-Macias and Luke, 2002). Studies on the MASW method have been extended to areas of utilization of higher modes (Xia et al., 2003; Beaty et al., 2002; Beaty and Schmitt, 2003), determination of near-surface Q (Xia et al., 2002c), optimization of field parameters of data acquisition (Zhang et al., in press), and deployment of autojuggie (Steeples et al., 1999) with the MASW method (Tian et al., 2003a and 2003b). However, we still face the fundamental question: what is the resolution power of high-frequency surface wave data/models. Lacking a certain resolution power, high-frequency surface wave data/models would be meaningless. Without understanding the resolving power of the MASW techniques, our ability to solve geological problems with the MASW techniques would not be clearly defined. Understanding the model resolution in inversion of Rayleigh wave phase velocities is critical in applying the MASW method to near-surface geological/geophysical problems. Xia and Chen (2003) introduced a concept of a smear matrix that explained why the vertical resolution of S-wave velocity profile obtained by inversion of Rayleigh wave data varies. The smear matrix clearly showed that errors in measured data limits the vertical resolving power of Rayleigh wave data. Xia and Chen (2003) concluded that the vertical resolution of the MASW model can be increased by increasing the accuracy of measured data. They also concluded that modeling results based on the layered earth model can provide a measure of the vertical resolution of the MASW technique in near-surface applications. They suggested that it is necessary to perform the forward modeling of high-frequency Rayleigh waves during the designing phase of a data acquisition to define the upper limits of the possible error level. Measured data with errors below this error level secure an inverted model possessing a certain vertical resolution that is sufficient for geological interpretation.

The MASW data are acquired as other geophysical surveys with an active source such as electromagnetic survey, electrical survey, Spectrum Analysis of Surface Waves survey (SASW, Stokoe et al., 1989), with the source and the receiver usually not placed at the same location. The horizontal resolution of geophysical models derived from these data is normally limited by the distance between the source and the receiver. In some cases, the separation between the source and the receiver is relatively small compared to the dimension of a specific geological problem, so the demand for improved horizontal resolution is relatively weaker. For certain geophysical techniques, however, the demand for improving horizontal resolution is very strong. MASW data acquisition requires certain source-receiver offsets to allow Rayleigh waves to fully develop into plane waves (Park et al., 1999; Zhang et al., in press). Specific source-receiver offsets are also required for acquiring enhanced Rayleigh waves and generating high-resolution images of dispersion curves. A new technique (Xia et al., 1998; Miller et al., 1999) combined the MASW method with a standard CDP (common depth point) roll-along acquisition format (Mayne, 1962) to generate 2-D S-wave velocity sections. This technique possesses a very high potential for applications in urban geophysical settings due to its high signal-to-noise ratio (Xia et al., 2004). However, because S-wave velocities are averaged values of the materials between the source and the last receiver, a process that reduces horizontal resolution, applications of the method in near-surface geophysics are limited.

In this study, we specifically discuss a generalized inverse technique for increasing the horizontal resolution of 2-D S-wave velocity sections obtained by the MASW method. Optimistic results from real-world data demonstrate the feasibility of this technique.

DOI:10.1190/1.1845123

Increasing horizontal resolution by inversion

Unblurred model

Menke (1984, p. 172) showed an example of an image enhancement. Let us consider that a one-dimensional camera records brightness along a line and assume that the camera moves parallel to the line. If the camera moves through three scene elements during an exposure, each camera element records the average of three neighboring scene brightnesses (Figure 1). If the contribution of three neighboring scene brightnesses is assumed to be equal, a relationship between scene elements (brightnesses) and camera pixels (records) can be described by the equation, $\mathbf{c} = \mathbf{Gs}$, where $\mathbf{c}$ is a vector of the camera pixels with a dimension of N and is called blurred model, $\mathbf{s}$ is a vector of scene elements with a dimension of M (M = N+2) and is called unblurred model, and $\mathbf{G}$ is the data kernel with the following form,

$$\mathbf{G} = \frac{1}{3}\begin{bmatrix} 1 & 1 & 1 & 0 & 0 & \dots & 0 \\ 0 & 1 & 1 & 1 & 0 & \dots & 0 \\ & & & \vdots & & & \\ & & & \vdots & & & \\ 0 & 0 & 0 & 0 & 1 & 1 & 1 \end{bmatrix}.$$

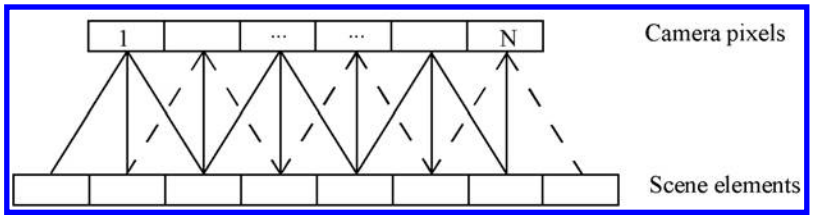

Figure 1. When a camera moves through three scene elements during an exposure, each camera pixel records the average brightness of three neighboring scene elements. There are two more unknowns than the number of data (From Menke, 1984).

The system $\mathbf{c} = \mathbf{Gs}$ is undetermined. The minimum length solution can be found by generalized inversion as $\mathbf{s} = \mathbf{G}^T [\mathbf{GG}^T]^{-1}\mathbf{c}$.

From this example, first, we understand that the data kernel $\mathbf{G}$, in fact, is a weighting matrix. The previous $\mathbf{G}$ is the equal weighted matrix. It is obvious that the data kernel $\mathbf{G}$ is determined subjectively. Based on different geophysical data and their accuracy, the data kernel may be determined differently. For the given example, we can define the data kernel proportional to 1/d (d is the distance from the camera to the screen) so the second nonzero element of each row in the data kernel will be a little larger than its neighboring elements on the same row. By doing that, we may obtain different unblurred model. Second, the condition number of matrix $[\mathbf{GG}^T]$ is normally very large so its inverse is unstable, especially when M is relatively large (> 100).

To stabilize the inverse processing, we first modify the data kernel in the following form

$$\mathbf{G} = \begin{bmatrix} 1 & 0 & 0 & 0 & 0 & \dots & 0 \\ 1/4 & 1/2 & 1/4 & 0 & 0 & \dots & 0 \\ 0 & 1/4 & 1/2 & 1/4 & 0 & \dots & 0 \\ & & & \vdots & & & \\ & & & \vdots & & & \\ 0 & 0 & 0 & 0 & 1/4 & 1/2 & 1/4 \\ 0 & 0 & 0 & 0 & 0 & 0 & 1 \end{bmatrix}.$$

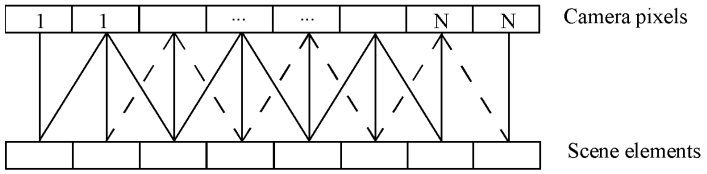

Figure 2. A modified setting of camera pixels and scene elements. Two "fake" pixels are added at each end of the camera pixels as input data.

We add one row in the beginning of the matrix and one row in the end matrix. Extra rows in the beginning and the end of the matrix represent the data extrapolation from the beginning and the end of the data set. The above matrix represents the simplest way to handle the extrapolation, i.e. to set the extrapolated data with the same as the first or the last data point (Figure 2). This modification allows the data kernel to be fully ranked theoretically, i.e. $R(\mathbf{G}) = M$. Second, we define the data kernel weighted unequally. The element in the center of the non-zero elements of $\mathbf{G}$ will be the largest and the non-zero elements on end will be the smallest. The smallest value is also the increment between weighting coefficients so that the elements between the smallest and the largest coefficients change gradually. Physically, by doing this so, we put higher weights on the data in the middle compared to the ones toward the edges. It is not only reasonable to put more weight on the data close to the center of transmitter and receiver(s) than rest of data, but clearly this weighting strategy also increases the values of the diagonal elements of matrix $\mathbf{G}$ and in this manner it improves the condition number of $\mathbf{G}$, which numerically stabilizes the inversion.

DOI:10.1190/1.1845123

The unblurred model **s** can be calculated by **s** = **Hc**, where **H** is the generalized inverse of **G**. Using the singular value decomposition technique (Golub and Reinsch, 1970), we can write $\mathbf{G} = \mathbf{U}\,\Lambda\,\mathbf{V}^T$ and the unblurred model $\mathbf{s} = \mathbf{Hc} = \mathbf{G}^T[\mathbf{G}\mathbf{G}^T]^{-1}\mathbf{c} = \mathbf{V}\,\Lambda^{-1}\,\mathbf{U}^T\mathbf{c}$, where **U** and **V** are semi-orthogonal matrices, and Λ is the diagonal matrix. The stability of the inverse matrix **H** can be achieved by introducing a damping factor in the diagonal matrix Λ^{-1}. The choice of the damping factor is really an "art" work of the inverse "game." This is why Claerbout (1992, p. 82) thought choosing a damping factor is a subjective matter. We selected the singular value of matrix **G** where the second derivative respect to its order index reaches the highest value as a damping factor to smooth the inverse with no firm theoretical basis. There probably are other better ways to determine the damping factor.

Real-world example

We applied the inverse technique discussed in the previous section to MASW data acquired in Andalusia, Alabama in 1999 (Miller and Xia, 1999). The data were collected along a dirt road within the Conecuh National Forest where sinkholes were present in close proximity (Figure 3). Data were recorded by a 60-channel Geometrics StrataView seismograph with forty-eight 4.5 Hz vertical component geophones separated by 4 ft and a Rubberband Assisted Weight Drop (RAWD) (built at the Kansas Geological Survey) as the source on 8 ft spacing. The nearest offset was 30 ft in hopes of mapping subsurface up to 100 ft of depth. Data were acquired from both directions along the dirt road. A total of 40 shots were collected in each direction in the CDP roll-along format. After determination of Rayleigh-wave phase velocities and inversion of each shot gather, we can generate 2-D S-wave velocity sections (Xia et al., 1998). Figure 4a shows a 2-D section with source location at lower station numbers pushing the geophone array forward and Figure 4b shows a section with the source at positions of higher station numbers pushing the geophone array backward. We expected both sections to be very similar to each other. In fact, they are different. The striking low velocity "bulls eyes" located around station 3057 and 3090 at a depth of 30 ft that are associated with nearby sinkholes. These low velocity features in Figure 4a were clearly different from corresponding ones in Figure 4b. The main reasons that caused the difference are that an S-wave velocity profile at each station was averaged (blurred) within a horizontal distance of 192 ft and sources at different locations.

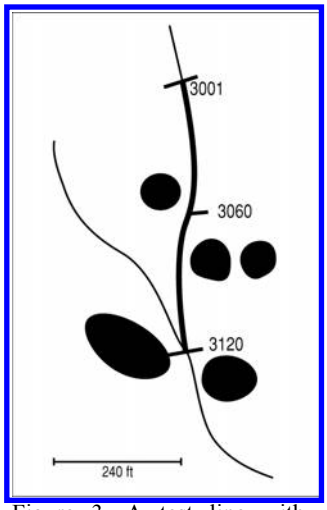

Figure 3. A test line with sinkholes.

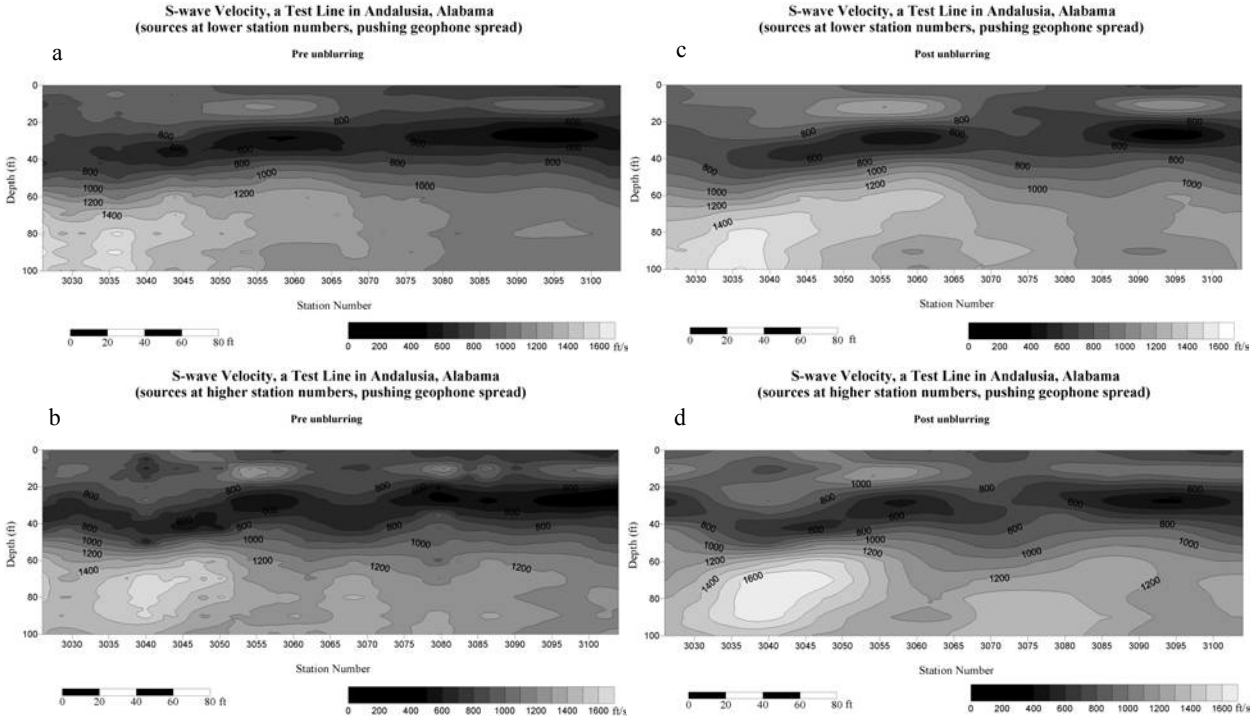

Figure 4. Blurred S-wave velocity models (a) and (b) and unblurred S-wave velocity models (c) and (d) by the inversion.

We defined the data kernel with the smallest element of 0.0069 to the largest 0.0833 with an increasing rate of 0.0069 and extrapolated the eleventh and twelfth data points from the first and last data points, respectively. Because the S-wave velocity model of Figure 4 consisted of 14 layers, we applied the inverse technique to the S-wave velocity model of Figure 4 layer by layer with the median of the singular values as a damping factor. After unblurring processing by the inversion, two velocity features in Figure 4c possess patterns similar to the corresponding ones in Figure 4d, especially the low-velocity feature around station 3090.

Conclusions

The unblurring processing discussed in this paper is a simple and effective way to improve horizontal resolution, especially for high-frequency surface wave data acquired in the CDP format. After unblurring, the horizontal resolution with source spacing could be achieved in the MASW S-wave velocity sections. This technique can also be applied to other geophysical data acquired with an active source (a transmitter) and receiver(s) being separated to improve their horizontal resolution.

Acknowledgements

We appreciate Mary Brohammer for her assistance in manuscript preparation.

References

Beaty, K.S., Schmitt, D.R., and Sacchi, M., 2002, Simulated annealing inversion of multimode Rayleigh wave dispersion curves for geological structure*: Geophys. J. Int*., 151**,** 622–631.

Beaty, K.S., and Schmitt, D.R., 2003, Repeatability of multimode Rayleigh-wave dispersion studies, *Geophysics*, v. 68, no. 3, 782-790.

Calderon-Macias, C., and Luke, B., 2002, Inversion of Rayleigh wave data for shallow profiles containing stiff layers: Technical Program with Biographies, SEG, 72ed Annual Meeting, Salt Lake City, UT, 1396-1399.

Claerbout, J.F., 1992, Earth soundings analysis: Processing versus inversion: Blackwell Scientific Publications, Boston.

Golub, G.H., and Reinsch, C., 1970, Singular value decomposition and least-squares solution: *Num. Math*., 14, 403-420.

Ivanov, J., Park, C.B., Miller, R.D., Xia, J., Hunter, J., Good, R.L., and Burns, R.A., 2000, Joint analysis of surface-wave and refraction events from river-bottom sediments: Technical Program with Biographies, SEG, 70th Annual Meeting, Calgary, Canada, 1307-1310.

Mayne, W. H., 1962, Horizontal data stacking techniques: Supplement to *Geophysics*, 27, 927-937.

Menke, W., 1984, Geophysical data analysis—Discrete inversion theory: Academic Press, Inc., New York.

Miller, R.D., Xia, J., Park, C.B., and Ivanov, J., 1999, Multichannel analysis of surface waves to map bedrock: *The Leading Edge*, 18, 1392-1396.

Miller, R.D., and Xia, J., 1999, Feasibility of seismic techniques to delineate dissolution features in the upper 600 ft at Alabama Electric Cooperative's proposed Damascus site, Interim Report: Kansas Geological Survet Open-file Report 99-3.

Park, C.B., Miller, R.D., and Xia, J., 1999, Multichannel analysis of surface waves: *Geophysics*, 64, 800-808.

Stokoe II, K. H., Rix, G. J., and Nazarian, S., 1989, In situ seismic testing with surface wave: Processing, XII International Conference on Soil Mechanics and Foundation Engineering, 331-334.

Tian, G., Steeples, D.W., Xia, J., Miller, R.D., Spikes, K.T., and Ralston, M.D., 2003a, Multichannel analysis of surface wave method with the autojuggie: *Soil Dynamics and Earthquake Engineering,* v. 23, no. 3, 243-247.

Tian, G., Steeples, D.W., Xia, J., and Spikes, K.T., 2003b, Useful resorting in surface wave method with the autojuggie: *Geophysics,* v. 68, no. 6, 1906-1908.

Steeples, D.W., Baker, G.S., and Schmeissner, C., 1999, Toward the autojuggie: Planting 72 geophones in 2 sec: *Geophysical Research Letters*, 26, 1085-1088.

Xia, J., Miller, R.D., and Park, C.B., 1998, Construction of vertical section of near-surface shear-wave velocity from ground roll: Technical Program, The Society of Exploration Geophysicists and The Chinese Petroleum Society Beijing'98 International Conference, 29-33.

Xia, J., Miller, R.D., and Park, C.B., 1999, Estimation of near-surface shear-wave velocity by inversion of Rayleigh wave: *Geophysics*, 64, 691-700.

Xia, J., Miller, R.D., Park, C.B., Hunter, J.A., Harris, J.B., and Ivanov, J., 2002a, Comparing shear-wave velocity profiles from multichannel analysis of surface wave with borehole measurements: *Soil Dynamics and Earthquake Engineering*, v. 22, no. 3, 181-190.

Xia, J., Miller, R.D., Park, C.B., Wightman, E., and Nigbor, R., 2002b, A pitfall in shallow shear-wave refraction surveying: *Journal of Applied Geophysics*, v. 51, no. 1, 1-9.

Xia, J., Miller, R.D., Park, C.B., and Tian, G., 2002c, Determining *Q* of near-surface materials from Rayleigh waves: *Journal of Applied Geophysics*, v. 51, no. 2-4, 121-129.

Xia, J., Miller, R.D., Park, C.B., and Tian, G., 2003, Inversion of high frequency surface waves with fundamental and higher modes: *Journal of Applied Geophysics*, v. 52, no. 1, 45-57.

Xia, J., and Chen, C., 2003, Model resolution of gross Rayleigh wave data: Technical Program with Biographies, SEG, 73rd Annual Meeting, Dallas, TX, 1243-1246.

Xia, J., Chen, C., Li, P.H., and Lewis, M.J., 2004, Delineation of a collapse feature in a noisy environment using a multichannel surface wave technique: *Geotechnique*, v. 54**,** no. 1, 17-27.

Yilmaz, O., and Eser, M., 2002, A unified workflow for engineering seismology: Technical Program with Biographies, SEG, 72nd Annual Meeting, Salt Lake City, UT, 1496-1499.

Zhang, S.X., Chan, L.S., and Xia, J., in press, The selection of field acquisition parameters for dispersion images from multichannel surface wave data: *Pure and Applied Geophysics.*

DOI:10.1190/1.1845123